RSC Advances

ROYAL SOCIETY OF CHEMISTRY

www.rsc.org/advances

RSC Advances

RSCPublishing

ARTICLE

Liquid-liquid phase separation and its effect on the crystallization in polylactic acid /poly (ethylene glycol) blends

Cite this: DOI: 10.1039/xoxxoooooox

Received ooth January 2012,
Accepted ooth January 2012

DOI: 10.1039/xoxxoooooox

www.rsc.org/

Yafang Xu, Wei Yu* and Chixing Zhou

Miscibility in blends of polylactic acid (PLA) and poly (ethylene glycol) (PEG) was investigated by means of differential scanning calorimetry (DSC), polarized optical microscopy (POM) and rheology with specifically designed thermal procedure. Direct observation of phase separated morphology via phase contrast optical microscopy is difficult because of the quite close refractive index of two components. Liquid-liquid phase separation (LLPS) was confirmed by appearance of two glass transitions after the sample been annealed at low temperatures (95~125°C). Moreover, the accelerated crystallization rate after the sample been annealed at high temperatures (140~160°C) also indicate the existing of LLPS according to the fluctuation assisted nucleation mechanism. An upper critical solution temperature (UCST) type of phase diagram was constructed via combination of DSC and rheological methods. Furthermore, the effects of LLPS on the kinetics of subsequent crystallization of PLA in blends with 15wt% PEG and 30wt% PEG were investigated. Considering the complex effect of LLPS on crystallization, we proposed a new model that integrates the Lauritzen-Hoffman theory and the self-concentration theory to account for the influence of miscibility on the crystallization in blends with different thermal histories. It is suggest that acceleration or deceleration of LLPS on the subsequent crystallization in highly asymmetric system depends on the interplay between the fluctuation assisted nucleation and the variation of mobility during LLPS.

1. Introduction

In the last twenty years, biodegradable polymers have attracted much more attention as popular awareness of exhausting petroleum resource and the long degradation period of petroleum-based polymers. Polylactic acid (PLA) is one kind of aliphatic polyesters that can be made from renewable resources.[1, 2]However, some drawbacks like slow crystallization rate, inherent brittleness and poor thermal resistance limit PLA for a wider application.[1] It has been reported that these shortages can be overcome by adding nanoparticles[3-6] and/or other component.[7-12] Wherein, poly (ethylene glycol) (PEG) is one of the most studied modifiers of PLA, which can depress glass transition temperature, enhance elongation at break and accelerate crystallization.[4, 9, 13-17] Generally, physical properties of blend are strongly dependent on the degree of miscibility and the crystallinity of the components. The earlier reports claimed that PLA/PEG blends could be completely miscible or partially miscible according to the number of glass transitions.[13, 15, 16]This criteria was somewhat arbitrary as some later researches revealed that two glass transitions could also be found in miscible blends with large dynamic asymmetry.[18, 19] Lai et al.[9] reported the blends, with PLA Mw= 200000 and PEG Mw=2000, were thermodynamically miscible throughout the entire range of composition above the melting point of PLA as they calculated a negative Flory-Huggins interaction parameter. In some cases, the intermolecular interaction plays an important role in the miscibility, the seemingly hydrogen bonding in PLA/PEG blends can be actually neglected due to the absence of hydrogen bonding band from infrared spectra.[20] Lai [9] also claimed the hydrogen bonding is expected to form between PEGs themselves as they found a lower level compatibility in PLA/PEG (2-OH) than PLA/PEG (2-CH_3). Another related factor is the solubility parameterδ. δ of PLA and PEG are in the range of 9.5-9.8 meaning a good compatibility, but it not the decisive role in phase behaviour especially in mixtures with significant difference in molecular structure and molecular weight.[20] The large dynamic asymmetry between PLA and PEG (big difference in T_g) can generate a quite different molecular dynamics at the same temperature, and this divergence of chain

Advanced Rheology Institute, Department of Polymer Science and Engineering, Shanghai Jiao Tong University, Shanghai, P. R. China. E-mail: wyu@sjtu.edu.cn; Tel: +86-21-54743275

mobility enhances with the decrease of temperature. Actually, only a few studies reported on the phase behaviour of PLA/PEG blend. Hu et al.[21] focused on the aging process and phase separation at ambient temperature. Up to date, the compatibility between PLA and PEG in the temperature regime above melting point of PEG are still not clear. Recently, the interplay between liquid-liquid phase separation and crystallization has received much more attention as it provides an efficient way to modulate the final phase morphology by control the level of phase separation and crystallization. Tanaka and Nishi [22, 23] investigated PCL/PS blend and found local liquid-liquid phase separation at the growth front of spherulites during crystallization. Han and co-workers have investigated the competition dynamics of LLPS and crystallization[22-25] and the influence of LLPS on the subsequent crystallization.[26] In turn, the crystallization kinetics can indicate the behaviour of LLPS. For example, Wang et al.[27] constructed phase diagram for HDPE/LLDPE blends by investigating the effect of LLPS on the following crystallization. They estimated binodal curve through monitoring crystallization kinetics and spinodal curve from crystal-decorated phase morphologies. Most recent researches considered dynamic asymmetry of components in liquid-liquid phase separation.[28, 29] In spite of these advances, the interpretations about the effect of LLPS on crystallization are mainly limited in a more qualitative way,[30-32] for better to control blend morphology and structure, the quantitative explanations are need.

In this paper, we will illustrate liquid-liquid phase separation of PLA/PEG from the effect of annealing on the variation of glass transition temperature (at low annealing temperature, T_{anneal}) and on the crystallization behaviour (at high T_{anneal}), from which the phase diagram is constructed. Furthermore, we intend to provide a quantitative insight into the effect of liquid-liquid phase separation on the subsequent crystallization. Hoffman and Miller [33] have introduced the concept of reptation to interpret the crystallization of entangled polymer, where the crystal growth rate was constrained by the mobility of chain segment. Miscibility of the second component not only changes the activation energy of chain motion, but also greatly alters the absolute value of monomer friction coefficient as illustrated by the self-concentration model.[18] Therefore, we proposed a new model, which combines the Lauritzen-Hoffman model and the Self-Concentration model (LH-SC), to describe the crystallization kinetics in crystalline polymer-rich phase and/or miscible blends.

2. Experimental section

2.1 Materials and sample preparation

PLA used in this work is NatureWorks® product 2002D. The semicrystalline grade resin comprises around 4% D-Lactide and the monomer content is less than 0.3wt%. It has a weight-average molecular weight about 2.0×10^5g/mol and a polydispersity of 1.75.[34] Polyethylene glycol (PEG) with a molecular weight of 10^4g/mol was obtained from Sinopharm Chemical Reagent Co., Ltd, P. R. China. PLA and PEG were dried at 40°C for 12h under vacuum before mixing. Blends with different compositions were mixed in chloroform, and the weight fraction indicates the content of PEG. The solutions were casted on glass plates, solvent was removed firstly by evaporation at ambient for 3 days, and then further dried in a vacuum oven at 40°C until a constant weight to reach. It is noted that the preparing temperature is below the melting points of PLA and PEG, crystallization may take place. However, all tests in this work were carried out after eliminating thermal history at 180°C for 5min. It is found that the glass transition behaviours (both the transition temperature and the width of transition) are identical for samples with different annealing time (5min and 50min) at 180°C, which means 5min is sufficient for samples to become homogeneous.

2.2 Differential scanning calorimetry (DSC) analysis

DSC (TA Instruments Q2000) was used to measure glass transition temperature and investigate isothermal crystallization behaviour of blends with different thermal history. The effect of annealing on glass transition was studied by procedure I (in Scheme 1). A piece of sample about 5 mg was heated to 180°C and held for 5min, then the temperature was decreased to the annealing temperature Tanneal (between 95°C and 125°C) and held for tanneal (three hours). Followed by rapidly quenched to -80°C and kept for 5 min, the sample was finally heated to 180°C at 10°C /min to determine the glass transition temperature. For blends without annealing, the sample was quenched from 180°C directly to -80°C, glass transition temperature was detected in the following heating procedure. The effect of annealing on isothermal crystallization was studied via the procedure II (in Scheme 1). The sample was annealed at 140°C for 2h, the subsequent crystallization temperature Tc was set between 90°C and 110°C. After the completion of crystallization, the sample was heated to 180°C again to determine melting point. For blends crystallized from molten state, the sample was quenched directly to T_c, and then heated to 180°C at 10°C /min.

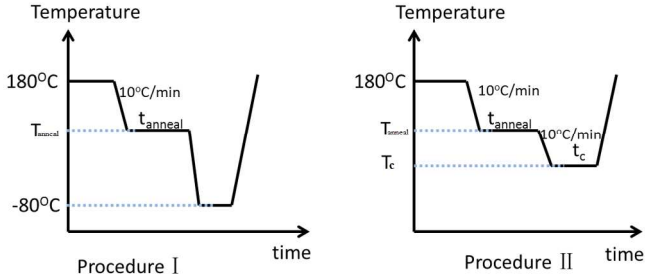

Scheme 1: Annealing and crystallization procedures of PLA/PEG blends.

2.3 Polarizing Optical Microscopy (POM)

Polarizing optical microscope (Leica DM LP, Leica Microsystems GmbH, Germany) equipped with hot stage (LK-600PH, Linkam, UK) was used to investigate growth dynamics of crystals. The sample was firstly cooled from 180 °C to T_{anneal} (140°C) holding for different time tanneal (0.5h, 1h and 2h) and then quenched to T_c (120°C) for isothermal crystallization. Crystallization of PLA was monitored isothermally by a Sony video camera at appropriate interval time and the growing radius of crystals were measured by Scion Image software.

2.4 Rheological measurements

Dynamic rheological experiments were carried out on a Gemini 200HR rotational rheometer (Malvern Instruments, UK) with parallel plate geometry of 25 mm in diameter. Samples for rheological measurement were obtained by compressing molding of the prepared blends into a sheet of thickness about 1 mm at 180°C under 5MPa. Two kinds of rheological measurements were performed. One is isothermal dynamic time

sweeps after high-temperature annealing under the frequency 1 rad/s and strain 1% to study the crystallization process. The variation of viscosity with time during crystallization was obtained. The other one is isothermal frequency sweeps in the range of 1~100 rad/s under a given strain amplitude of 5%, which was in the linear viscoelastic regime as determined previously by strain sweep. The temperature of frequency sweep ranged from 120°C to 180°C with 10°C intervals, from which the temperature dependence of zero shear viscosity was obtained. The total time for dynamic frequency sweep was very short (several minutes) as compared to the development of crystallization and/or LLPS, so the blends can be reasonably considered as in homogeneous state during test.

3 Results and discussions

3.1 Effect of annealing on glass transition

Fig. 1a shows the last heating can of 15wt% blend after been annealed at 95~125 °C for three hours (procedure I). The cold crystallization has disappeared and the melting enthalpies of PLA (in Table 1) are almost identical, which indicate three hours is sufficient for PLA to complete crystallization. Of particular interest here is the change of glass transition. Only one glass transition is observed in the sample without annealing, while two distinct glass transitions can be clearly identified from the derivative heat flow curves of annealing samples in Fig. 1b and Fig. 1c in high temperature range and low temperature range, respectively. At high temperature range, there is a partial overlap of the glass transition of PLA and the melting process of PEG (Fig. 1a). The glass transition of 15wt% blend is about 27-39 °C, and the melting point of PEG in the blend is above 50°C, even so, they can be well separated in the derivative heat flow curves (Fig. 1b).

Two glass transition temperatures are usually found either in phase separated blends or in miscible blends with large dynamic asymmetry.18 After annealing, the crystallization of PLA would make PEG concentration increased if the amorphous domain is still in miscible, which will reduce the glass transition temperature of PLA. This is inconsistent with the experimental observations. There are two possible reasons for the shift of PLA's T_g to higher temperature. One is due to the liquid-liquid phase separation (LLPS) between PLA and PEG. LLPS results in a decrease of PEG concentration in the PLA-rich domains, which can lead an increase of PLA's T_g. The other possible reason is the formation of so-called "rigid amorphous phase" (RAF) during crystallization, which has higher Tg than the "mobile amorphous phase" (MAF).[35] The formation of RAF always bring a widening of glass transition, while LLPS results in a narrowing of glass transition. The width of transition for the annealed sample is estimated to be about 16K narrowed than without annealing 20K. In addition, the crystallization of PEG in 15wt% blend is difficult due to the low concentration. Even after the crystallization of PLA, the concentration of PEG in amorphous is not sufficient high (about 20wt %) to crystallize if there is no LLPS. It is highly probable that the crystallization of PEG in the blend after annealing happens in the PEG-rich domains. This is consistent with the appearance of the second glass transition at low temperature (Fig. 1c), which is ascribed to the glass transition of PEG-rich phase. All these phenomena supports the happening of LLPS during annealing.

3.2 Dependence of glass transition on composition

From the above discussion, the liquid-liquid phase separation and the level of phase separation can be reflected by the variation of glass transition. Since the glass transition is directly related to the blend composition, it is possible to evaluate phase compositi-

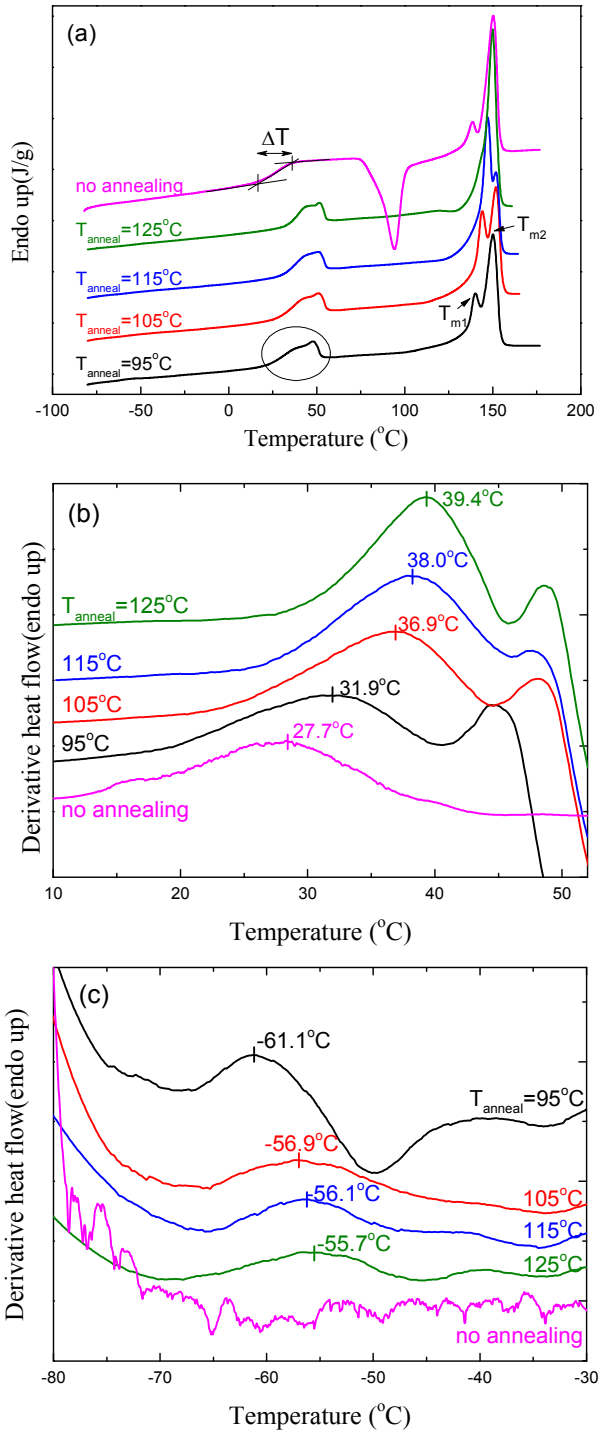

Fig.1 DSC heating curves for 15wt% PEG after been annealed at different temperatures for 3 hours (a) and derivative heat flow at high-temperature region (b) and at low-temperature region (c).

on from the T_g-concentration dependence. Thermal diagrams of a set of blends directly quenched from 180 °C are measured and

shown in Fig. 2. Due to the fast quench, possible liquid-liquid phase separation is prevented in measurement. Only one T_g is observed and decreased from 59°C for pure PLA to 25°C for 15wt% blend. In the blends with PEG content higher than 70wt%, only a weak and broad transition at very low temperature found. The glass transitions of PEG-dominant blends at low temperature range and of PLA-dominant blends at high temperature range can be seen more clearly in the insets. Pure PEG glass transition temperature is hardly observed under our experimental condition and quoted from literature as -67 °C.[36]

Table 1 DSC data together with the corresponding average volume concentration of PEG in two phases

T_{anneal} (^oC)	$\Delta H_{m,PLA}$ (J/g)	$T_{g,1}$ (^oC)	$T_{g,2}$ (^oC)	$\phi_{PEG,1}$[a] (v%)	$\phi_{PEG,2}$[b] (v%)
No annealing	33.5	/	25.9	/	16.6
95	36.5	-61.1	31.9	88.0	11.2
105	36.5	-56.9	36.9	84.4	8.8
115	36.6	-56.1	38.0	82.3	7.9
125	36.9	-55.7	39.4	80.5	7.1

[a,b] the average volume concentration of PEG was calculated from glass transition temperature using self-concentration model.

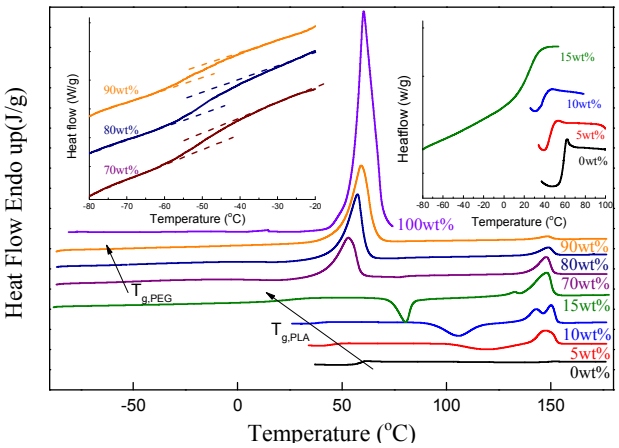

Fig.2 DSC trace for PLA/PEG blends with heating scan of 10°C /min. Arrows are added to guide the eyes for the variation of glass transition temperature with composition.

The glass transition temperature as a function of PEG content is shown in Fig. 3, where the PEG content denotes the volume fraction in amorphous phase. Because the crystallization of PEG and PLA cannot be avoided even under fast cooling, the average concentration of PLA and PEG in amorphous should be corrected by subtracting the fraction of crystallinity as follows, $\phi_{PEG}^{am} = \frac{w_{PEG} - \Delta H_{m,PEG}/\Delta H_{m,PEG}^0}{\rho_{PEG}} \cdot \left(\frac{w_{PEG} - \Delta H_{m,PEG}/\Delta H_{m,PEG}^0}{\rho_{PEG}} + \frac{w_{PLA} - (\Delta H_{m,PLA} + \Delta H_{cc,PLA})/\Delta H_{m,PLA}^0}{\rho_{PLA}} \right)^{-1}$ (1)

Enthalpies of PEG melting in PEG-dominant blends as well as PLA cold crystallization and melting in PLA-dominant blends are summarized in Table 2, the corrected average volume concentrations of PEG are also listed. We adopt the self-concentration model of Lodge-McLeish[18] to describe the glass transition temperature in blends. The self-concentration model is

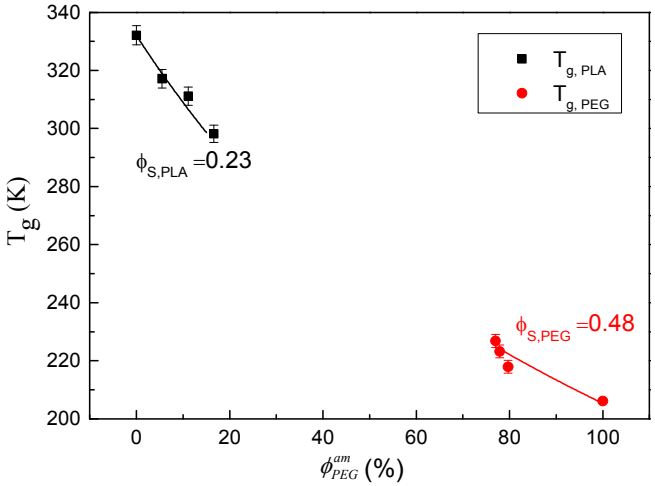

Fig. 3 The dependence of glass transition temperature on PEG content. The solid lines are fitting curves by the self-concentration model with $\phi_{s,PLA} = 0.23$ and $\phi_{s,PEG} = 0.48$, respectively.

based on the realization that local composition for monomer of type A is different from the average bulk composition as the surrounding environment is enriched with A component due to chain connectivity. The effective local concentration $\phi_{eff,i}$ of component i can be calculated from self-concentration ϕ_s and the bulk composition ϕ by

$$\phi_{eff,i} = \phi_{s,i} + (1 - \phi_{s,i})\phi_i \quad (2)$$

Self-concentration is suggested to be the ratio between the self-volume occupied by the chain segments V_s and the reference volume V_{ref}, i.e. $\phi_S = C_\infty M_0 / K\rho N_{AV} V_{ref}$,where C_∞ is the characteristic ratio of polymer, K is the number of backbone bonds per polymer repeat unit, ρ is the polymer density, N_{AV} is the Avogadro's number and M_0 is the repeat unit molar mass. The choice of reference volume is a little arbitrary, and it is suggested to use the volume occupied by Kuhn segment[18] or to be taken as a fitting parameter. The effective glass transition temperature ($T_{g,eff}$) of component i is related to its local concentration in a volume comparable to the size of chain segments instead of the average bulk concentration. The Fox equation is suggested to correlate the effective concentration and the effective glass transition temperature:

$$\frac{1}{T_{g,eff,i}} = \frac{\phi_{eff,i}}{T_{g,i}} + \frac{1 - \phi_{eff,i}}{T_{g,j}} \quad (3)$$

where $T_{g,i}$ and $T_{g,j}$ are glass transition temperature for pure component i and j , respectively. Such model implies that two glass transitions can be observed even in miscible blends as long as big difference in components' glass transition. Moreover, it also suggests that the change in the glass transition is referred to the variation of local environment of chain segment, which is related to the miscibility of components in polymer blends. Eq. (2) and (3) are used to fit the glass transition temperature as shown in Fig. 3, where the self-concentration of PLA and PEG are taking as the fitting parameter. The best fit gives ϕ_s 0.23 for PLA and 0.48 for PEG, which are close to the theoretical calculations (0.2 for PLA and 0.36 for PEG). Using the fitted self-concentration, we can calculate the mean concentration from glass transition temperature and the results are shown in Table 1.

Table 2 Parameters in the heating scan of DSC curves and the corrected PEG average volume concentration

Sample (wt% PEG)	$\Delta H_{cc,PLA}$ (J/g)	$\Delta H_{m,PLA}$ (J/g)	$\Delta H_{m,PEG}$ (J/g)	$T_{g,PLA}$ (°C)	$T_{g,PEG}$ (°C)	Φ_{PEG}^{am} * (%)
0	-	0.3	-	59.2	-	0
5	17.5	17.5	-	45.5	-	5.6
10	26.8	26.9	-	38.4	-	11.1
15	33.3	33.5	-	25.9	-	16.6
70	0.5	17.1	59.9	-	-49.9	77.9
80	-	7.9	90.0	-	-46.3	77.0
90	-	1.6	126.2	-	-55.2	79.7

* The referred $\Delta H_{m,PLA}^0$ is 93.7 J/g, 5 and $\Delta H_{m,PEG}^0$ is 220 J/g .[37] ρ_{PEG} is 1.128 g/cm^3 and ρ_{PLA} is 1.27 g/cm^3.

3.3 Effect of annealing on crystallization

To study the effect of annealing on crystallization, the thermal history of procedure II in scheme 1 is adopted. Fig.4 shows crystal radius of 5wt% and 15wt% blends that recorded at 120 °C after samples been annealed at 140 °C for different time. No crystal observed on polarized optical microscopy when annealed at 140 °C. Linear growth of crystals is seen in Fig.4, the slope gives the overall crystal growth rate, which is around 2.05 μm/min for 5wt% blend in all cases. For 15wt% blend, the growth rate increases with the previous annealing time, i.e., 6.36μm/min, 6.63μm/min and 7.25 μm/min for 0h, 1h, and 2h, respectively. The acceleration of crystallization after annealing can be attributed to the LLPS.[27, 31] One explanation is that the probability of crystallizable polymer adsorbing onto the crystal growth front is higher than that in the miscible blend, similar to the "poisoning" effects from diluent.[38] The other one is ascribed to the increase of the nucleation rate in the concentration gradient region (or interface), where the diffusion-induced aligned segments may attach themselves to the interface and become nuclei or precursor of nuclei for crystallization. [39]

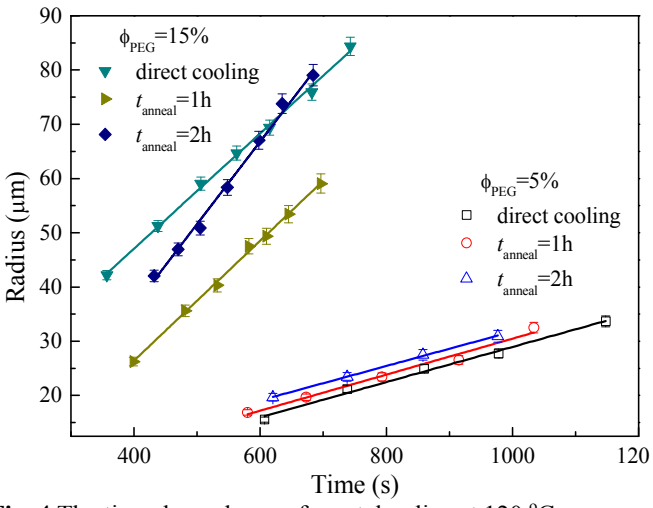

Fig. 4 The time dependence of crystal radius at 120 °C.

To elucidate the effect of annealing temperature on the subsequent crystallization, the rheological method was adopted due to its high sensitivity to crystallization. The variation of complex viscosity during crystallization is monitored on a rotational rheometer by dynamic time sweep. The lower limit of annealing temperature should ensure no generation of crystals and the upper limit should avoid thermal degradation. The whole process was operated under quasi-quiescent condition to avoid the influence from shear flow. Three blends of 15wt%, 30wt% and 50wt% were investigated. Fig.5a shows the variation of normalized complex viscosity of 15wt% blend after been annealed at 140 °C, 150 °C and 155 °C for different period of time. The monotonically increase of viscosity denotes the happening of crystallization. The time when the normalized complex viscosity becomes two is taken as the onset of crystallization. The shorter onset crystallization time the faster crystallization. It can be seen from Fig.5a that the onset crystallization time decreases with the extension of annealing at 140°C and 150°C. When the annealing temperature increase to 155°C, the speedup of the following crystallization almost disappeared. Similar trend can be found in 30wt% blend (Fig.5b). The vanished acceleration of crystallization at higher annealing temperature means weaker LLPS and indicates UCST-type of phase diagram.

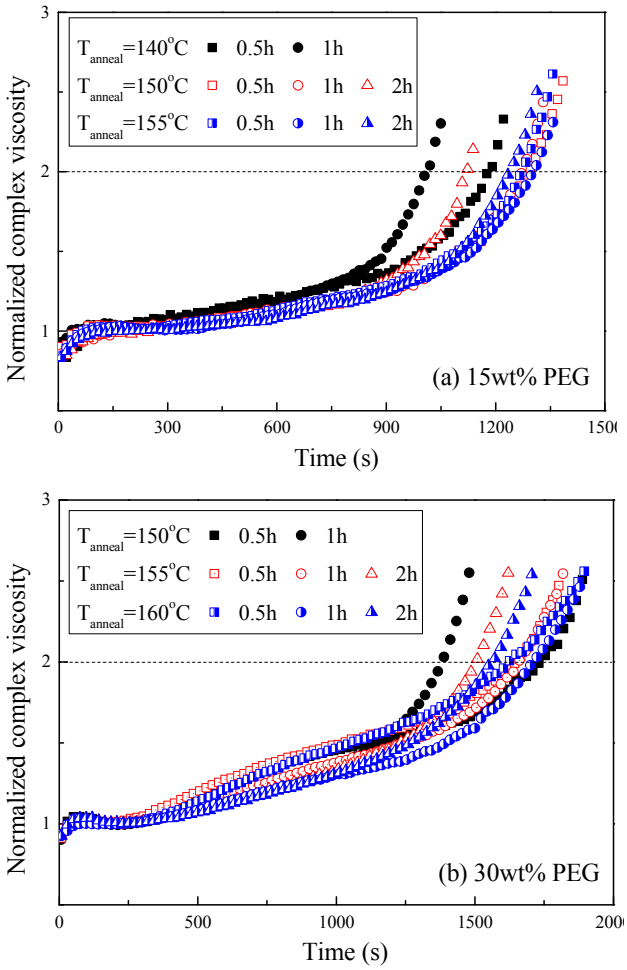

Fig. 5 The normalized complex viscosity as a function of time at Tc=120°C for samples with different thermal treatments. (a) 15wt% PEG blend has been annealed at 140 °C, 150 °C and 155 °C; (b) 30wt% PEG blend has been annealed at 150 °C, 155 °C and 160 °C.

3.4 Phase diagram

Phase diagram is an important information for partially miscible polymer blends. The phase boundary is usually obtained by measuring the discontinuity of some physical properties with temperature, such as cloud point temperature or transmittance temperature,[40] the storage modulus of bulk[41] or the change of heat flow.[42] Since the two components in this work possess nearly identical refractive index ($R_{I,PLA}$=1.44-1.46, $R_{I,PEG}$=1.46),[1, 36] it is difficult to detect their liquid-liquid phase separation temperature via optical ways. In contrast, crystallization of PLA is relatively easy to monitor by either optical microscopy or rheology method. Moreover, in the presence of LLPS, the glass transition temperature and the kinetics of crystallization can be altered, which also provide indirect ways to infer binodal boundary of LLPS.

The phase diagram of PEG/PLA blend is shown in Fig. 6, which is composed of two parts. At high annealing temperatures (above 140 °C), liquid-liquid phase separation is the only phase transition.We identified binodal point as the annealing temperature above which the annealing treatment has no influence on the subsequent crystallization. The transition temperatures are about 150~155 °C, 160~165 °C and 155~160 °C for 15wt%, 30wt% and 50wt% blend, respectively. Such method to construct phase boundary is based on the interplay between crystallization and phase separation. At low temperatures (95~125°C), LLPS and crystallization can happen simultaneously, and the interplay between them determines the concentration distribution and morphology development. When the blend was annealed at low temperatures, the results of crystallization and LLPS change the local concentration in amorphous PLA-rich domains and amorphous PEG-rich domains, which is revealed by the change of glass transitions. The mean concentration in different domains have been estimated from the self-concentration model as shown in Table 1, and they are taken as approximated phase boundary in Fig. 6. Such phase boundary is probably not the thermodynamic equilibrium one because the actual extent of LLPS depends on the competition with crystallization. At 125°C, where the crystallization is slow and LLPS has sufficient time to develop in spite of the lower thermodynamic driving force. On the contrary, crystallization under 95 °C is much faster, the system is quickly frozen and the development of LLPS is limited. Then, it is expected that more deviation from the equilibrium would be exist at lower temperatures.

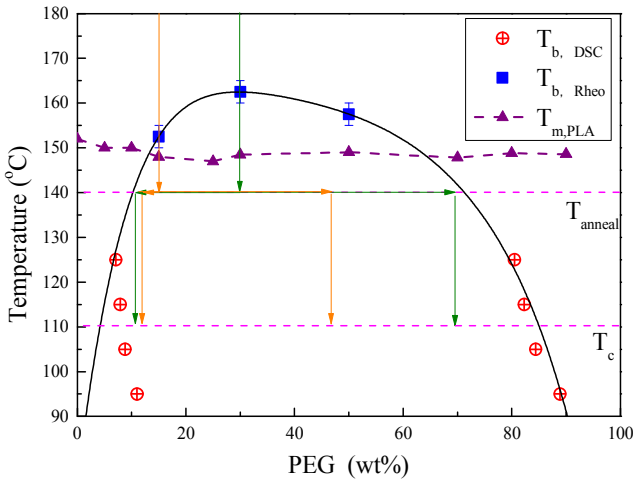

Fig. 6 Phase diagram for PLA/PEG determined from rheology and DSC. The solid line is the fitting curve of a polynomial equation. The arrows denote the evolution of concentration during two-step quench tests will discuss in next section.

3.5 Effect of annealing on the kinetics of crystallization

In the blends with simultaneous LLPS and crystallization, it is interesting to know the specific variation of crystallization kinetics due to the presence of liquid-liquid phase separation. To this end, the crystallization behaviour of 15wt% and 30wt% blends were studied by DSC using thermal history as procedure II in Scheme 1. Fig.7 shows a set of overall heat flow with time at different crystallization temperatures for samples with one-quench and two-quench treatment, where one-quench denotes the sample is quenched directly from melt (180 °C) to T_c, while two-quench denotes the sample is firstly quenched from melt to the annealing temperature (140°C) for 2h and then to the crystallization temperature.

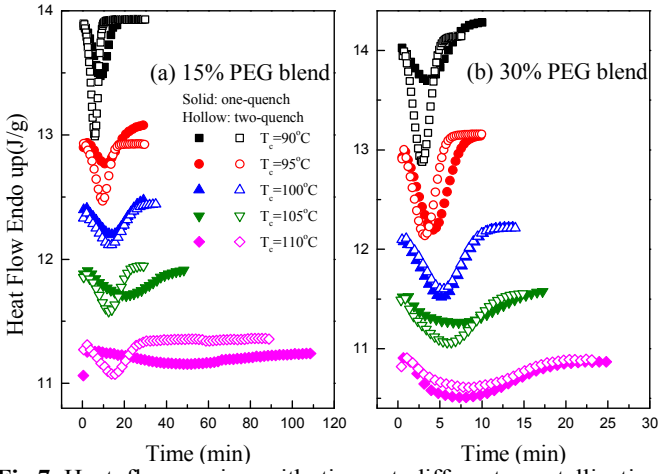

Fig.7 Heat flow varies with time at different crystallization temperatures for (a) 15wt% PEG and (b) 30wt% PEG. The filled symbols are samples directly quenched from melt and the hollow symbols are samples quenched firstly to 140°C for 2h then quenched to T_c.

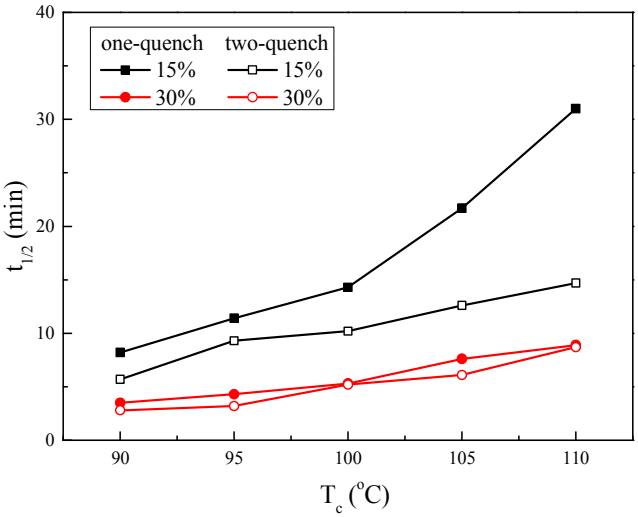

Fig.8 Relationship of $t_{1/2}$ with T_c for one-quench test and two-quench test.

The crystallization rate is clearly displayed in the graph of the half-crystallization time $t_{1/2}$ with T_c as shown in Fig. 8. For the same thermal treatment, $t_{1/2}$ becomes smaller as temperature decreases, which is attribute to the enhancement of nucleation at low temperatures. Meanwhile, as compared with one-quench, $t_{1/2}$ of 15wt% blend decreased obviously in two-quench procedure, which is consistent with the previous POM and rheological results. For 30wt%blend, the effect of LLPS on crystallization is less obvious. At the same annealing temperature (140 °C), the thermodynamic driving force of LLPS is larger in 30wt% blend than in 15wt% blend due to the deep quench. It is possible that the separated PLA-rich domains and PEG-rich domains in 30wt% blend has component concentration much closer to the phase boundary when annealing for the same time (as indicated by arrows in Fig. 6). Therefore, the PLA-rich domains in 30wt% blend has a lower content of PEG and then a higher glass transition temperature, that is, a weaker chain mobility for PLA crystallization. Both the effect of "fluctuation assisted nucleation" and the chain mobility depends on the level of phase separation. Comprehensive understanding of crystallization needs detailed analysis of thermodynamic parameters.

Actually, the effect of LLPS on the crystallization in blends with different PEG content and different thermal histories rely on both the transportation ability and the nucleation ability. According to the Lauritzen-Hoffman secondary nucleation theory,[33] the growth rate of linear polymer crystal with the chain folding is expressed as:

$$G = G_0 \exp\left[\frac{-U^*}{R(T_c - T_\infty)}\right] \exp\left[\frac{-K_g}{T_c \cdot (\Delta T) \cdot f}\right] \quad (4)$$

where G_0 is a pre-exponential term that contains all the factors that do not depend much on temperature, U^* is the activation energy for transportation of segments to the crystallization site, R is the universal gas constant, T_c is the crystallization temperature and T_∞ is the temperature at which all the motions associated with the viscous flow are frozen, and is defined as $T_\infty = T_g - C$, C is a constant (30K). ΔT is supercooling $T_m^0 - T_c$, f is the correction factor defined as that accounts for the change in heat of fusion as the temperature is decreased below T_m^0. K_g is the nucleation rate given as $K_g = nb\sigma\sigma_e T_m^0 / k\Delta H_m^0$,[33] where k is the Boltzmann constant, b is the thickness of the stem added on the substrate, σ is the lateral surface free energy, σ_e is the free energy of folding, ΔH_m^0 is the enthalpy of fusion. In this theory, the growth rate G were governed by the energy required to transport segments across the solid-liquid interface and by the nucleation rate variations occurring at high degree of undercooling. In the crystallization of homopolymer, both the activation energy and the surface free energy determine the kinetics. However, these parameters might change due to the presence of the second partially miscible component.

As the intrinsic differences in chain mobility between the components, the presence of PEG could alter the activation energy for transportation of PLA. However, both the LLPS and the crystallization make PEG concentration continuously varied with time, it is difficult to determine dynamic activation energy for transportation during crystallization but we can still estimate on the average concentration of PEG. At crystallization temperatures (near and below about T_g+100 °C), the dependence of activation energy on temperature shifts from Arrhenius to 'Vogel' behaviour,[33] where U^* can be determined from zero shear viscosity η_0

$$U^* = \frac{Rd(\ln \eta_0)}{d(1/T)} \quad (5)$$

Dynamic frequency sweep at different temperatures (120-170 °C) were measured on rheometer, zero shear viscosity is fitted by Carreau-Yasuda model. Fig. 9 displays the variation of zero shear viscosity with the reciprocal of temperature for blends from 0wt% to 30wt%, the linear dependency between $\ln \eta_0$ and $1/T$ can be found, the activation energy for transportation of segments is determined from the slope according to Eq. 5. The values are 109.8kJ/mol, 107.1kJ/mol, 83.5kJ/mol and 80.0kJ/mol for PEG content 0wt%, 5wt%, 15wt% and 30wt%, respectively. Although some of experiments are investigated in two-phase regime of phase diagram (Fig. 6), the effect from LLPS can be ignored during rheological measurements because the terminal relaxation is fast for all testing samples, dynamic frequency sweeps were done within several minutes. The results show that the activation energy for transportation does

not change greatly for 15wt% and 30wt%. Therefore, it is expected that the variation of U^* due to the addition of PEG is not the main cause for the difference in the crystallization.

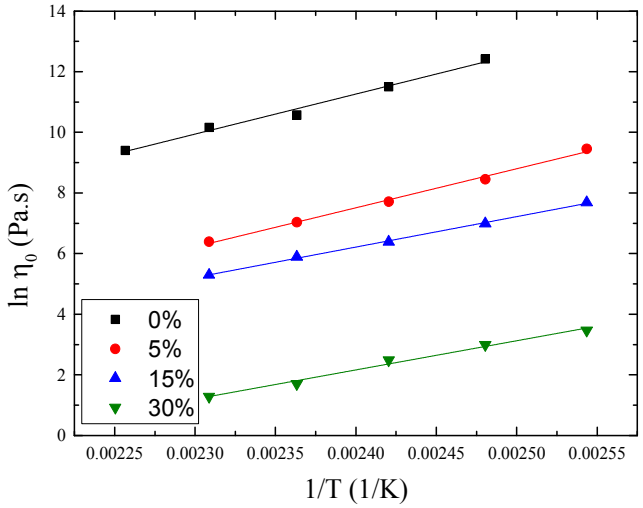

Fig. 9 Zero shear viscosities of PLA/PEG blends versus the reciprocal of temperatures, whose slopes are used to determine the activation energy for transportation.

Furthermore, the chain dynamics are important for crystallization and phase separation. Hoffman and Miller[33] have conjoined reptation theory and surface nucleation theory to analyze crystallization, where the pre-exponential term in Eq. 4 is inversely proportional to the monomeric friction coefficient ζ_0, i.e., $G_0 = G_0'/\zeta_0$. In reptation theory, the monomeric friction coefficient determines the whole chain dynamics. Since the local dynamics of each component in blend can be reflected from the distance from the glass transition temperature, it is suggested that actual friction coefficient can be evaluated using WLF equation with the effective glass transition temperature according to self-concentration model,[18]

$$\ln\left[\frac{\zeta_i(\phi)}{\zeta_{g,i}}\right] = -\frac{c_1^g\left[T - T_{g,eff,i}(\phi)\right]}{c_2^g + T - T_{g,eff,i}(\phi)} \quad (6)$$

where c_1^g and c_2^g are constants, $\zeta_{g,i}$ denotes the friction coefficient at glass transition temperature. It is important to notice that self-concentration model considers the scale of Kuhn segment length, which is different from the scale of monomer. We assume here that the dynamics at both length scales have the same temperature dependence, and Eq. (6) can also suitable for monomeric friction coefficient. Combining the SC model for the monomeric friction and L-H theory for secondary nucleation and growth, we have

$$\ln G + \frac{U^*}{R(T_c - T_\infty)} - \frac{c_1^g\left[T - T_{g,eff,i}(\phi)\right]}{c_2^g + T - T_{g,eff,i}(\phi)} = \ln G_0' - \ln\zeta_{g,i} - \frac{K_g}{fT_c\Delta T} \quad (7)$$

The third term on the left hand of Eq. 7 represents the correction of growth rate by the change of chain dynamics. The nucleation rate K_g is obtained from the slope of the left side of Eq. 7 with $1/fT_c\Delta T$. In this work, attention is paid to the PLA-rich domains as they are able to crystallize in our investigated temperature. Thus, only the values of c_1^g and c_2^g of PLA need to be determined and they are supposed to be the same as those of pure PLA. The time-temperature superposition principle is established for pure PLA. Through fitting the temperature dependence of horizontal shifting factor by WLF equation, c_1^g and c_2^g are obtained as 19.3 and 48.4, respectively. $T_{g,eff,i}(\phi)$ is the effective glass transition temperature of PLA-rich phase, which can be readily calculated if known the composition of PLA-rich phase after LLPS. As the extent of LLPS is not easily to determine, we make a crude approximation that phase separation reaches to the apparent binodal boundary (about 10wt% PEG, referring to Fig. 6) in two-quench for both 15wt% and 30wt% blends, while PEG concentration in one-quench is as prepared composition. The plot of LH-SC model (Eq. 7) is shown in Fig.10, where the absolute value of slope is used to determine K_g. It is seen that the nucleation constant K_g decreases from 1.6×10^6 Pa^2 in one-quench to 1.4×10^6 Pa^2 in two-quench for 15wt% blend. While, K_g of 30% PEG blend changes very slightly. If the crystallization regime is not changed, we can suppose the lateral surface free energy is also unchanged. Then, the free energy of folding in 15wt% PEG blend decreased about 13% in two-quench test as compared to one-quench , while the change in 30wt% PEG blend is negligible. This result manifests directly the effect of fluctuation assisted nucleation on the free energy of chain folding.

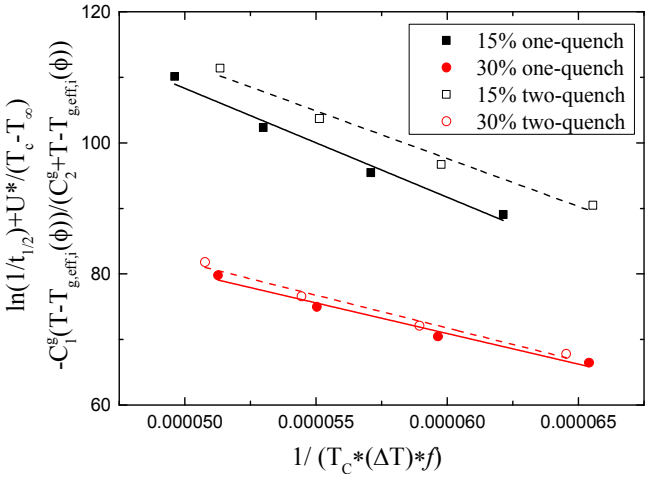

Fig. 10 Plots of LH-SC model for PLA/PEG blends containing 15% and 30% PEG with different thermal history. Solid lines denote the linear fit of one-quench data, dash lines denote the linear fit of two-quench data.

Therefore, the apparent crystallization speed is an interplay between the mobility factor and the folding free energy. When non-crystallizing component has a higher T_g, LLPS will cause a decrease of effective T_g of the crystallizing polymer, which results in faster chain motion. Such effect has the same positive contribution to crystallization speed as the fluctuation assisted nucleation, which decreases the folding free energy. In contrast, when non-crystallizing component has a lower T_g, LLPS will cause an increase of effective T_g of the crystallizing polymer, which slows down the chain motion. The apparent crystallization speed will be determined by the dominating factor, either the change of mobility or the change of folding free energy. Then it is possible that LLPS can result in either faster crystallization or slow crystallization. In most previous studies on the relationship between LLPS and crystallization using polyolefin blends, dynamic asymmetry is not important

and LLPS always induces faster crystallization. In the present study, although PLA/PEG is a typical dynamical asymmetric system, the decrease of chain mobility during phase separation is not significant enough to slow down the crystallization. The apparent crystallization after weak LLPS is still dominated by the fluctuation assisted nucleation.

4. Conclusions

The liquid-liquid phase separation and its effect on the crystallization in the blend of PLA/PEG were studied. Although most studies state that PLA and PEG are miscible, evidences are found here to justify the liquid-liquid phase separation between two components. One evidence is the appearance of two glass transition temperatures after annealing at relatively low temperatures (95~125 ^{o}C), where the increased glass transition of PLA and the appearance of glass transition of PEG suggest liquid-liquid phase separation during annealing. Quai-equilibrium phase compositions are determined from the steady state glass transition temperatures of separated phases based on the dependence of glass transition temperature on composition. The other evidence is the acceleration of crystallization after samples been annealed at high temperature region (140~160 ^{o}C), and the lowest annealing temperature at which has no effect on the subsequent crystallization is deemed as binodal point for the investigated blend. Then, the phase diagram is constructed from the effect of annealing on T_g and the effect of annealing on crystallization.

The effect of LLPS on the subsequent crystallization was studied on 15wt% and 30wt% blends. The isothermal half-crystallization time becomes smaller in two-quench test of 15wt% blend, but little change in 30wt% blend. The difference comes from the extent of LLPS, where both the concentration fluctuation and the chain dynamics affect the crystallization. We suggest to combine the Lauritzen-Hoffman model with the self-concentration model to separate the effect of chain dynamics and concentration fluctuation. It is found that no obvious variation of folding free energy in 30wt% blend in both situations, while the free energy of chain folding in 15wt% blend decreases about 13% in two-quench test, which manifests quantitatively the effect of fluctuation assisted nucleation by chain stretching in the interfacial region. The combination of L-H model and S-C model in partially miscible blend also implies the competition between fluctuation assisted nucleation and LLPS induced mobility `variation in blends with high dynamic asymmetry. It is possible that LLPS can accelerate or decelerate the apparent crystallization speed depending on the glass transition temperatures of crystallizable component and non-crystallizable component, while the deceleration effect still needs further experiments to justify.

Acknowledgements

This work is supported by the National Natural Science Foundation of China (No. 50930002) and National Basic Research Program of China (No. 2012CB025901). W. Yu is supported by the Program for New Century Excellent Talents in University and the SMC project of Shanghai Jiao Tong University.

References

1. D. Garlotta, *Journal of Polymers and the Environment*, 2001, **9**, 63-84.
2. K. Madhavan Nampoothiri, N. R. Nair and R. P. John, *Bioresource Technology*, 2010, **101**, 8493-8501.
3. L. Jiang, J. Zhang and M. P. Wolcott, *Polymer*, 2007, **48**, 7632-7644.
4. H. Li and M. A. Huneault, *Polymer*, 2007, **48**, 6855-6866.
5. R. Liao, B. Yang, W. Yu and C. Zhou, *Journal of Applied Polymer Science*, 2007, **104**, 310-317.
6. J. You, W. Yu and C. Zhou, *Industrial and Engineering Chemistry Research*, 2014, **53**, 1097-1107.
7. L. Zhang, C. Xiong and X. Deng, *Polymer*, 1996, **37**, 235-241.
8. O. Martin and L. Avérous, *Polymer*, 2001, **42**, 6209-6219.
9. W.-C. Lai, W.-B. Liau and T.-T. Lin, *Polymer*, 2004, **45**, 3073-3080.
10. E. Piorkowska, Z. Kulinski, A. Galeski and R. Masirek, *Polymer*, 2006, **47**, 7178-7188.
11. C. Liu, S. Lin, C. Zhou and W. Yu, *Polymer (United Kingdom)*, 2013, **54**, 310-319.
12. J. You, L. Lou, W. Yu and C. Zhou, *Journal of Applied Polymer Science*, 2013, **129**, 1959-1970.
13. C. Nakafuku and M. Sakoda, *Polymer Journal*, 1993, **25**, 909-917.
14. C. Nakafuku, *Polymer Journal*, 1996, **28**, 568-575.
15. M. Sheth, R. A. Kumar, V. Davé, R. A. Gross and S. P. McCarthy, *Journal of Applied Polymer Science*, 1997, **66**, 1495-1505.
16. J. M. Yang, H. L. Chen, J. W. You and J. C. Hwang, *Polymer Journal*, 1997, **29**, 657-662.
17. Z. Kulinski and E. Piorkowska, *Polymer*, 2005, **46**, 10290-10300.
18. T. P. Lodge and T. C. B. McLeish, *Macromolecules*, 2000, **33**, 5278-5284.
19. A. N. Gaikwad, E. R. Wood, T. Ngai and T. P. Lodge, *Macromolecules*, 2008, **41**, 2502-2508.
20. H. Younes and D. Cohn, *European Polymer Journal*, 1988, **24**, 765-773.
21. Y. Hu, Y. S. Hu, V. Topolkaraev, A. Hiltner and E. Baer, *Polymer*, 2003, **44**, 5711-5720.
22. H. Tanaka and T. Nishi, *Physical Review Letters*, 1985, **55**, 1102.
23. H. Tanaka and T. Nishi, *Physical Review A*, 1989, **39**, 783.
24. H. Wang, K. Shimizu, H. Kim, E. K. Hobbie, Z.-G. Wang and C. C. Han, *The Journal of Chemical Physics*, 2002, **116**, 7311.
25. W. Shi and C. C. Han, *Macromolecules*, 2011, **45**, 336-346.
26. X. Zhang, Z. Wang, X. Dong, D. Wang and C. C. Han, *The Journal of Chemical Physics*, 2006, **125**, 024907-024910.
27. S. Wang, C. Wu, M.-Q. Ren, R. M. Van Horn, M. J. Graham, C. C. Han, E. Chen and S. Z. D. Cheng, *Polymer*, 2009, **50**, 1025-1033.
28. W. Yu, R. Li and C. Zhou, *Polymer*, 2011, **52**, 2693-2700.
29. W. Yu and C. Zhou, *Polymer*, 2012, **53**, 881-890.
30. S. Wook Lim, K. Hee Lee and C. Hyung Lee, *Polymer*, 1999, **40**, 2837-2844.
31. J. Luo, Y. Liang, J. Yang, H. Niu, J.-Y. Dong and C. C. Han, *Polymer*, 2012, **53**, 2465-2475.
32. Z. He, Y. Liang, P. Wang and C. C. Han, *Polymer*, 2013, **54**, 2355-2363.
33. J. D. Hoffman and R. L. Miller, *Polymer*, 1997, **38**, 3151-3212.
34. J. Liu, L. Lou, W. Yu, R. Liao, R. Li and C. Zhou, *Polymer*, 2010, **51**, 5186-5197.
35. B. Wunderlich, *Progress in Polymer Science*, 2003, **28**, 383-450.
36. J. E. MARK, *Polymer Data Handbook,Oxford University Press*, 1999.
37. K. Pielichowski and K. Flejtuch, *Polymers for Advanced Technologies*, 2002, **13**, 690-696.
38. S. Z. D. Cheng, *Phase Transitions in Polymers: The Role of Metastable States, Elsevier*, 2008.
39. X. Zhang, Z. Wang, R. Zhang and C. C. Han, *Macromolecules*, 2006, **39**, 9285-9290.
40. C. Huang, J. Gao, W. Yu and C. Zhou, *Macromolecules*, 2012, **45**, 8420-8429.
41. R. Li, W. Yu and C. Zhou, *Journal of Macromolecular Science, Part B*, 2007, **46**, 1051-1062.
42. P. Van de Witte, A. Boorsma, H. Esselbrugge, P. J. Dijkstra, J. W. A. van den Berg and J. Feijen, *Macromolecules*, 1996, **29**, 212-219.

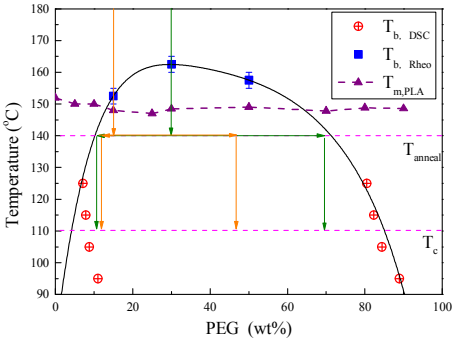

Phase diagram of PLA/PEG determined from rheology and DSC